ELSEVIER

Ecological Modelling 138 (2001) 173–191

ECOLOGICAL MODELLING

www.elsevier.com/locate/ecolmodel

Numerical modelling of the initial spread of sewage from diffusers in the Bay of Piran (northern Adriatic)

Vlado Malačič *

Marine Biological Station Piran, National Institute of Biology, Fornače 41, 6330 Piran, Slovenia

Abstract

A numerical model of initial dilution of sewage emerging from an orifice of a diffuser into stratified waters of the southern part of the Gulf of Trieste is presented. Municipial wastewater from the town of Piran empties into the sea from two diffusers at the end of adjacent submarine pipes (length 3.5 km), located at the open entrance of the shallow Bay of Piran (depth 21 m). First a numerical analysis of the hydraulics of each of the diffusers was developed to estimate the outflow through each of the diffusers' orifices. Second, a numerical model was developed for the initial rising of sewage plumes in a marine environment with a complicated stratification. The model follows the conservation laws of mass, momentum and buoyancy, integrated over the cross-section of a buoyant plume. The system of equations is solved with the Runge-Kutta method with adaptive step-size, which keeps the local error bounded. The model was calibrated with known semi-analytical expressions for a linearly stratified sea. A sensitivity analysis of the model was also completed. Model simulations demonstrated that the initial inclination of a buoyant jet has low influence on dilution, but a high influence on rise height. On the other hand, the discharge velocity has a relatively low impact on the rise height, but affects the dilution much more. The model also showed that in a calm sea with typical summer stratification, plumes, which emerge from orifices spaced at 10 m, remain well separated until they reach a layer of neutral buoyancy below the sea-surface.

Keywords: Initial dilution; Northern Adriatic; Coastal sea

1. Introduction

The treatment and subsequent spreading of sewage into shallow coastal seas is a serious problem in populated coastal areas. Today's demands for high quality sewage manipulation require biochemical (third stage) treatment, which usually follows mechanical treatment. The latter is at present the most common treatment in the coastal communities surrounding the Gulf of Trieste. Three towns along the southern coast of the gulf (Koper, Izola and Piran) are forced to meet high standards of sewage handling and are, therefore, preparing operative plans for the renewal, reconstruction and redesign of their sewage treatment. This study was prompted by these planned activities.

More than a decade ago, a study of the distribution of the sewage discharges around the Gulf

* Tel.: +386-56-746368; fax: +386-56-746367.
E-mail address: malacic@nib.si (V. Malačič).

0304-3800/01/$ - see front matter
PII: S0304-3800(00)00401-4

of Trieste (Olivotti et al., 1986) showed that about 23% of the sewage load arrived into the gulf from the southern (Slovenian) coast. Of the three communities only the town of Piran (7% of the sewage load) had a system of discharge, which was composed of two long submarine pipes, which ended with diffusers. The first submarine pipe, of external diameter 0.40 m, had been operative since 1976, when the sewage treatment plant commenced operation. It was designed for a maximum flow rate of 0.15 $m^3\ s^{-1}$, which was then believed to be adequate for excess loads (50 000 units during the tourist season). This diffuser will be denoted as the 1976 diffuser. Ten years of operation showed the need for the second pipe (external diameter 0.64 m), which was installed in 1987 alongside the existing pipe and will be referred to as the 1987 diffuser.

Several studies in the seventies and eighties monitored the plankton, nutrients and bentic communities around the 1976 diffuser (Avčin et al., 1979; Malej, 1980; Faganeli, 1982). They did not show any severe environmental deterioration due to sewage disposal. Recent studies examined the distribution of fluorometric signal in the wastewater near-field (Malačič and Vukovič, 1997), and among different nutrients that were analyzed in near-field samples, amonia was confirmed as a substance that followed the presence of bacteria in diluted wastewater (Mozetič et al., 1999).

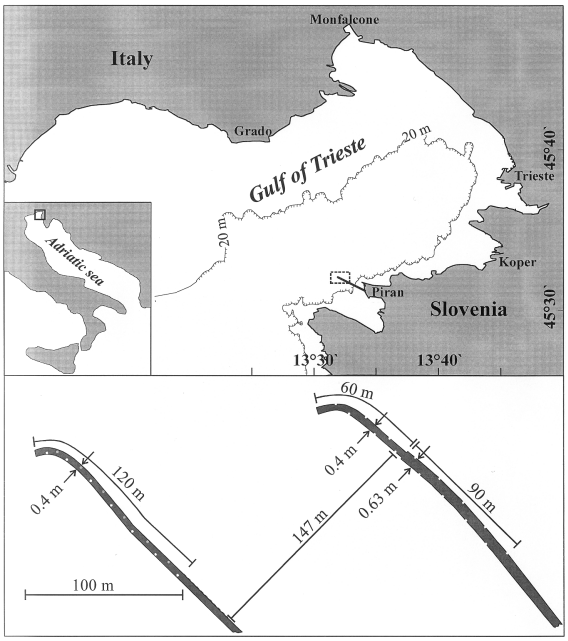

Fig. 1. Top, location of two diffusers (dashed rectangle) of the outfall in front of the Bay of Piran. Bottom, zoom on two adjacent diffusers.

Modeling the hydraulics of 1987 diffuser and the initial dilution in a homogeneous sea of 20-m depth was undertaken just before the installation of this diffuser (Lalić, 1987). In this paper a review of hydraulics was presented, in which the in situ particularities of the diffusers' structures were considered. More important, an accurate numerical model for the simulation of the initial spread of buoyant plumes, which emerge into a stratified sea is presented.

2. Study area

The Gulf of Trieste (Fig. 1) is a shallow (depth, 20 m) semi-enclosed gulf, with a flat bottom at the southern side. Exchange of water mass with the rest of the northern Adriatic Sea occurs through its opening at the western side.

The studied area is around the location of two adjacent sewage diffusers from the town of Piran (Fig. 1) at the southern entrance of the Gulf of Trieste. Diffusers are about 2.6 km away from the nearest coastal point (the tip of St. Madonna of the cape of Piran). Diffusers were installed about 1 m above the flat sea-floor. The length of the wider pipe (1987) L_I was 3250 m and of the narrower pipe (1976) L_{II} was 3650 m. The ratio of the internal pipe cross-section areas of two parallel pipes with internal diameters $D_I = 0.591$ m and $D_{II} = 0.375$ m, into which the sewage enters gravitationaly, was $S_I/S_{II} = 2.48$. The sewage flow arriving from the plant through a pipe of diameter 0.64 m was split with a 'V' element into two pipes, one of internal diameter D_I, and the other of diameter D_{II}. Both of these pipes ended in diffusers. Their ends were deflected westward (Fig. 1, bottom) due to the interference of fishermen (bottom trawler). Both diffusers were drilled with the alternating orifices of diameter $d = 0.1$ m at a

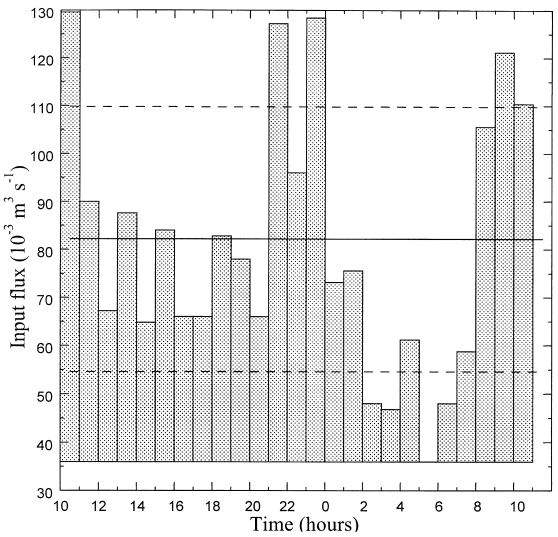

Fig. 2. Daily variations of the influx of sewage into the treatment plant on 10–11 February 1999. Since the level in a treatment basin can be taken as nearly constant, the inflow is a good representation of the outflow into the sea. The daily average of hourly flow rate $\langle\phi\rangle = 82.2 \times 10^{-3}$ m^3 s^{-1} (horizontal full line) with S.D. $(\phi) = 27.6 \times 10^{-3}$ m^3 s^{-1}, numerous $N = 26$. Dashed lines represent $\langle\phi\rangle \pm$ S.D. (ϕ).

distance $\Delta x = 10$ m. Unfortunately, both diffusers were also rotated with respect to the horizontal axis along the pipe; the 1976 diffuser had orifices at an angle of about 65° with respect to the horizontal axis, while the orifices of the 1987 diffuser were at an angle of about 30° from the horizontal axis (not shown in Fig. 1). This rotation slightly modified the hydraulic characteristics, as it will be seen from the simulations.

3. Hydraulics

3.1. Hydraulics of the discharge system

The discharge system was constructed in such a way that the sewage passed first through a single pipe from the collecting reservoirs (20.3-m above sea-level), which after 196 m divides into a 'V' junction. The two parallel pipes then led the sewage into the coastal sea about 3.5 km away. In calculations of the hydraulics of the diffusers we had encountered the obstacle of not knowing the flow rate of sewage through each of the two pipes.

From the hydraulics of a branched system of pipes, it follows that the ratio of flow-rates between the two branches yields (Douglass et al., 1979; Chadwick and Morfett, 1986).

$$\left(\frac{\phi_{II}}{\phi_I}\right) = \frac{S_{II}}{S_I}\left(\frac{L_I D_{II}}{L_{II} D_I}\right)^{1/2} \cong \frac{S_{II}}{S_I}\, 0.75 \cong 0.3, \qquad (1)$$

when the total flow rate of discharge from the reservoir $\phi = \phi_I + \phi_{II} = 0.1$, $\phi_I = 0.077$, and $\phi_{II} = 0.023$ m^3 s^{-1}. From the inspection of pipe fittings and elements over the whole discharge system we concluded that $\phi_{II}/\phi_I = 0.3 \pm 0.1$ under near-steady flow conditions.

Fig. 2 shows that the diurnal range of flow rate (93.6×10^{-3} m^3 s^{-1}) is higher than the mean daily value (82.2×10^{-3} m^3 s^{-1}) of hourly flow rate during the period of 10–11 February, 1998. The hourly outflow rate during the morning period was calculated out from ten records of the rotation rates of pumps at the input side of the treatment basins collected from 1996 to 1997. Its value was 0.12 ± 0.05 m^3 s^{-1}, and we let $\phi = 0.1$ m^3 s^{-1}.

3.2. Hydraulics of diffusers

To calculate spreading and dilution one first needs to know the flow rate through the orifices of diffusers. The hydraulics of diffusers has been treated by Fischer et al. (1979), and described by Brooks (1970).

There are two major differences between the two adjacent diffusers in the outfall system in Piran. First, it was ascertained by scuba-diving inspection that the 1976 diffuser was loaded with sludge, which blocked the operation of one-third of the diffuser toward the end-side. The 1987 diffuser was clear. Second, there is the difference in the diffusers' construction. The 1976 diffuser was composed of a single pipe, while the 1987 diffuser was composed of two pipes (Fig. 1). As was pointed out in the previous section, both diffusers were also rotated so that the orifices were not jetting the sewage horizontally. Therefore, since the 1987 diffuser carried the major part of sewage (3.3 times more than the 1976 diffuser), we will concentrate on the hydraulics of this diffuser.

The calculation begins at the end of the diffuser. Let there be the first orifice with the outflow rate q_1,

$$q_1 = C_D A\sqrt{2gE_1}, \tag{2}$$

where E_1 is the total head loss through the orifice; $A = \pi d^2/4$ is the cross-section area of the orifice; $g = 9.81$ m s^{-2} is the gravity acceleration, and C_D the discharge coefficient. The energy loss E_1 is chosen to be a tuning parameter so that the total flow rate through the diffuser matches the flow rate through the pipe, which is required. The 1987 diffuser has been repaired at its end by inserting a concrete cork with an orifice of the same diameter as the diameters of the other orifices. The energy losses at the end of this diffuser are due to sudden contraction (from diameter 0.591 m of the pipe to diameter 0.1 m of the orifice of the cork) and due to discharge into an infinite reservoir, which lead to the value of C_D in Eq. (2):

$$C_D = \frac{1}{\sqrt{1.5}} = 0.82, \tag{3}$$

which is higher than the value of C_D for other orifices, which are close to 0.63. For nth port ($n > 1$), according to laboratory results for Reynolds number $Re > 2 \times 10^4$ (Brooks, 1970),

$$C_D = 0.63 - 0.58\left(\frac{V_{n-1}^2}{2gE_n}\right). \tag{4}$$

The algorithm by which one would proceed with hydraulic calculus from $(n-1)$th orifice towards nth orifice will be outlined simply here; for the details the reader is referred to Brooks (1970), Fischer et al. (1979),

$$q_n = C_D A_n\sqrt{2gE_n}, \tag{5}$$

$$\Delta V_n = \frac{4q_n}{\pi D^2}, \tag{6}$$

$$V_n = V_{n-1} + \Delta V_n, \tag{7}$$

$$h_n = f\frac{L_n V_n^2}{2Dg}, \tag{8}$$

$$E_{n+1} = E_n + h_n + \left(\frac{\Delta\rho}{\rho}\right)\Delta z_n. \tag{9}$$

where $\Delta V_n = V_n - V_{n-1}$ is the velocity increment between the neighboring ports $n-1$ and n. Frictional head loss between nth and $(n+1)$th port, which are separated by distance L_n (10 m), is h_n, and $f = 0.019$ is the friction factor of the polyethylene pipe. A value for f has been chosen as the average value of the friction factors of the segments between orifices of the pipe, that were calculated according to Swamee and Jain (1976), Roberson and Crowe (1997). The elevation difference of neighboring ports is $\Delta z_n = z_{n+1} - z_n$, and $\Delta\rho/\rho$ is the relative difference between the surrounding density ρ_{a0} outside the nth port and the sewage density ρ. The hydraulic calculus is still accurate enough when we suppose for the sake of simplicity $\Delta\rho/\rho = 0.025$.

When the position of the flow contraction (from a pipe of diameter 0.63 m to a pipe of diameter 0.4 m) is reached between Nth and $(N+1)$th port ($N = 7$), then the following procedure needs to be inserted. First, the expression Eq. (8) is to be replaced with a similar one

$$h_N = f\frac{L_{N+1/2}V_N^2}{2Dg}, \tag{10}$$

and then proceed with

$$V_{N+1/2} = V_N\left(\frac{D_d}{D_u}\right)^2$$

$$h_{N+1/2} = h_N + f\frac{L_{N+1}V_{N+1/2}^2}{2gD_u} + K_L\frac{V_N^2}{2g}, \tag{11}$$

$$E_{N+1} = E_N + h_{N+1/2} + \left(\frac{\Delta\rho}{\rho}\right)\Delta z_N, \tag{12}$$

where $L_{N+1/2}$ is the spacing between the Nth port and the pipe's contraction (5 m); L_N (= 5 m) is the spacing between the $(N+1)$th port and the pipe's contraction, D_d is the downstream diameter, D_u the upstream diameter and $K_L = 0.444$ the coefficient of local head loss at sudden contraction (Chadwick and Morfett, 1986). Then again, the algorithm Eqs. (4)–(9) is to be followed back up for the wider part of the diffuser, where $n \geq N+1$, until the last orifice is reached.

It was mentioned in the previous section that both diffusers were rotated along their axis so that the orifices were no longer horizontal, giving a height difference Δz_n between the two neighboring orifices. It was found that there was a jump in the 1987 diffuser height of 0.5 m just next to the

pipe's contraction, where the pipe had been additionally weighted. Both effects, the diffuser rotation and differential immersion of the diffuser in a silt bottom induced 'corrections' of the heights of the orifices. The scuba diver's report is incomplete in the sense that it is unknown whether the height of the top of the pipe corresponds to the orifice which is above, or below, the mid-line of the pipe. Therefore, both situations were considered. The resulting flow rates q_n per port and the velocity V_n through a diffuser are plotted in Fig. 3. The hydraulics has been adjusted for the total flow rate $\phi_I = 0.100\ m^3\ s^{-1}$. Jumps of q_n and V_n at the location of the diffuser's contraction are clearly evident. Mean and S.D. of the discharge q per port are $(5.5 \pm 0.5) \times 10^{-3}\ m^3\ s^{-1}$, whereas without height variations $q = (5.5 \pm 0.2) \times 10^{-3}\ m^3\ s^{-1}$. We may estimate that the velocity of fluid u_0 emerging from the ports is, therefore, $u_0 = (0.70 \pm 0.06)\ m\ s^{-1}$ for $\phi_I = 0.100\ m^3\ s^{-1}$. When the division of the flow into two pipes is considered, the flow rate ϕ_I is decreased (e.g. to $0.070\ m^3\ s^{-1}$), and in rough approximation the discharge per port is decreased proportionally ($q = (3.85 \pm 0.4) \times 10^{-3}\ m^3\ s^{-1}$).

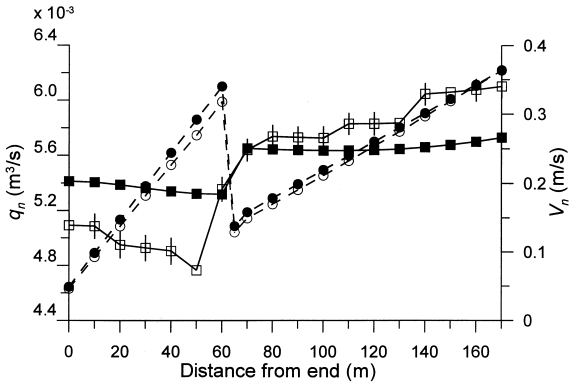

Fig. 3. Variations of discharge per port q_n (full lines) and velocity V_n (dashed lines) in diffuser 1987. All curves refer to the total flow rate $\phi_I = 0.100\ m^3\ s^{-1}$. For a diffuser without any variations in height (horizontal one) q_n is represented with full rectangles, and V_n with full circles. Empty rectangles (q_n) and empty circles (V_n) refer to a diffuser with variations in height due to differential immersion of the diffuser. Vertical bars represent variations of q_n and V_n due to diffuser rotation for 30° along its axis, small bars for V_n are masked by symbols.

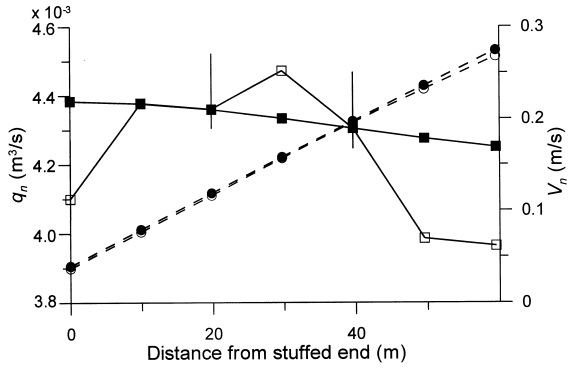

Fig. 4. Same as Fig. 3 for the diffuser 1976. All curves refer to the total flow rate $\phi_{II} = 0.030\ m^3\ s^{-1}$. Note that the distance is from the filled part of diffuser (about one-third of diffuser) and the whole diffuser is rotated 65° and tilted upward due to differential immersion (until March 2000). For the simulation seven active ports have been chosen.

The 1976 diffuser presents a problem, since its last one-third at the tip is filled with sludge (and silt). Moreover, the diver's report shows that this diffuser's differential immersion resulted in an upward tilt; the end of the diffuser is higher than the beginning by about 0.8 m over the 100-m length. It is not known exactly how many ports are operating, for the rough estimate seven orifices have been chosen.

When the inclination of the diffuser was considered in the hydraulic calculus of the 1976 diffuser (Fig. 4), the S.D. of the discharge per orifice was higher ($q_n = (4.3 \pm 0.2) \times 10^{-3}\ m^3\ s^{-1}$) than the S.D. of the discharge per port for a horizontal diffuser ($q_n = (4.3 \pm 0.05) \times 10^{-3}\ m^3\ s^{-1}$). The discharge velocity was then $(0.55 \pm 0.03)\ m\ s^{-1}$.

4. The initial dilution above diffuser

When choosing a direction in which a numerical model of initial dilution is to be developed, the characteristics of the existing ambient parameters and the geometry of the diffuser have to be investigated first, since they notably affect the spreading of sewage emerging from the diffusers' orifices.

As far as the ambient conditions are concerned in the shallow Gulf of Trieste (depth 22 m or less) it is important to notice that the gulf is character-

ized by large variations of stratification. During the summer, temperatures may vary from 15°C at the sea-floor up to 25°C at the sea-surface (Malačič, 1991), and salinity differences of up to 5 PSU are expected within the water column. Vertical variations of temperature and salinity during the season both contributed to enhanced vertical variations of density with depth (Malej et al., 1997). The 'bulk' buoyancy frequency of the water column, which may be approximated with $g\Delta\rho/(\Delta z\rho_{a0})$, spans from a near zero value in winter to 0.05 s^{-1} in summer (when it has been reasonably supposed for $\Delta\rho = 4.7$ kg m^{-3} over $\Delta z = 20$ m; $\rho_{a0} = 1027.8$ kg m^{-3}). Vertical alterations of local buoyancy frequency

$$N = \left[-g\left(\frac{d\rho_a}{dz}\right)\rho_{a0}^{-1} \right]^{1/2}, \quad (13)$$

where $\rho_a(z)$ is the ambient density and $\rho_{a0} = \rho_a(z = 0)$, are, therefore, much larger during the season.

For simplicity, we shall take for a length scale of the diffusers $L = 100$ m. Since the orifices are about 1 m above the bottom, we may take that the maximum height at which a buoyant parcel would travel, is $H = 20$ m. The latter may also be considered to be the maximum limit of the length scale of the height of a buoyant plume l_B.

4.1. Model equations

In the construction of a model of initial dilution and spreading of a buoyant plume the model fundamentals of Featherstone (1984) have been followed, in which values of model parameters were checked with a model calibration. The model runs using unevenly distributed data of depth-density pairs of ambient stratification and has an adaptive step-size algorithm to keep the local numerical error sufficiently small.

It is reasonable to suppose that the buoyant plume has a much higher turbulence intensity than the intensity of the stagnant surrounding sea, so the latter will be disregarded. The model simulates the steady spreading of a buoyant jet emerging into the stratified sea from a round port. The axisymmetric geometry of the problem allows the integration of equations of motion and continuity across the plume's section, which is orthogonal to the tangent of the route of the plume's core. Let the area of the cross-section of a buoyant jet be denoted by A, the following integral quantities are introduced,

$$\phi = \int_A u\, dA; \quad \Psi = \int_A \rho u\, dA; \quad M = \int_A u^2\, dA;$$
$$B = g\int_A \left(\frac{\Delta\rho}{\rho_{a0}}\right) u\, dA; \quad T = g\int_A \left(\frac{\Delta\rho}{\rho_{a0}}\right) dA, \quad (14)$$

where ϕ is the volume flux, Ψ the mass flux, M the specific momentum flux, B the buoyancy flux through the slice of a plume, and T is the specific buoyant force per unit length of a plume. Let the length of a path of a core be denoted by s; the dependence of all four fluxes on s is to be looked for. When the ambient current is ignored, there is no change of momentum in the horizontal direction, while in the vertical direction the buoyancy causes changes:

$$\frac{d}{ds}(M\cos\theta) = 0; \quad \frac{d}{ds}(M\sin\theta) = T, \quad (15)$$

where θ is the angle of inclination of a tangent of a plume's trajectory to the horizontal axis (Fig. 5). Volume and mass fluxes change along the trajectory due to entrainment of ambient fluid through the plume's side (Turner, 1986) of perimeter $2\pi b$ and height ds (Fig. 6):

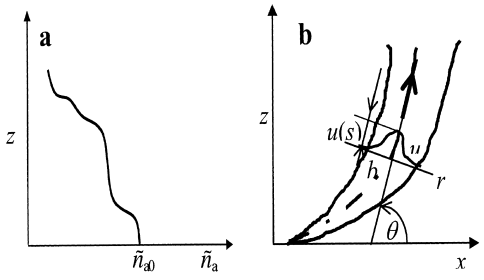

Fig. 5. (a) Sketch of a vertical profile of ambient density; (b) buoyant jet, which emerges from the coordinate origin. The radius at which the velocity falls to $1/e$ of the central value $u(s)$, is b.

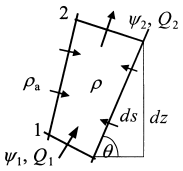

Fig. 6. Small element of a buoyant plume of length ds and density ρ, along which the entrainment of surrounding fluid changes the volume flux between cross-sections 1 and 2 for E ds, and the specific mass flux for $E\rho_a$ ds.

$$\frac{d\phi}{ds} = E = 2\pi b\alpha u(s), \tag{16}$$

radius b is the one at which the velocity falls to $1/e$ of the axis value; the entrainment parameter α ($\cong 0.08$) is the first of the model parameters which will be under examination; and $u(s)$ is the peak velocity at the center of a plumes's slice. The problem simplifies if the Gaussian variations of the velocity $u(r, s)$ and density deficit $\Delta\rho$ ($=\rho_a-\rho$) across the buoyant slice are supposed:

$$u(s,r) = u(s)e^{-r^2/b^2}; \quad \Delta\rho(s,r) = \Delta\rho(s)e^{-r^2/\lambda b^2}, \tag{17}$$

where a second model parameter λ has been introduced — it follows from observations (Fischer et al., 1979, Tables 9.2 and 9.3) that the cross-section profile of density deficit is wider than the profile of velocity; $\lambda \cong 1.2$. Considering Eq. (17) in Eq. (14) yields

$$\phi = \pi u(s)b^2(s); \quad M = \frac{\pi u^2(s)b^2(s)}{2}.$$

The rate of change of buoyancy flux along the trajectory is proportional to ϕ (see the Appendix A):

$$B = \frac{\pi g\lambda^2\Delta\rho(s)u(s)b^2(s)}{\rho_{a0}(1+\lambda^2)};$$

$$T = \frac{\pi g\lambda^2\Delta\rho(s)b^2(s)}{\rho_{a0}}. \tag{18}$$

$$\frac{dB}{ds} = \frac{g}{\rho_{a0}}\frac{d\rho_a}{ds}\phi. \tag{19}$$

It follows from this relation that B is constant, when the ambient is homogeneous ($d\rho_a/ds = 0$), regardless of changes of the volume flux along the path of a plume. This is an important property, which indicates that the solutions for $d\rho_a/ds <> 0$ will be close to the buoyant plume for which B is constant. When fluxes ϕ, M in B from Eq. (18) are inserted together with T in Eqs. (15), (16) and (19), the following system of equations is obtained:

$$\frac{d(u^2b^2)}{ds} = 2\alpha bu, \tag{20}$$

$$\frac{d(u^2b^2\cos\theta)}{ds} = 0, \tag{21}$$

$$\frac{d(u^2b^2\sin\theta)}{ds} = \frac{2g\Delta\rho}{\rho_{a0}}\lambda^2b^2, \tag{22}$$

$$\frac{d(\Delta\rho ub^2)}{ds} = \frac{(1+\lambda^2)}{\lambda^2}ub^2\frac{d\rho_a}{ds}. \tag{23}$$

In the system (Eqs. (20)–(23)) the core velocity $u(s)$ and the core density deficit $\Delta\rho(s)$ along the axis of the plume are, hereafter, denoted simply by u and $\Delta\rho$. This system has to be translated into a system of explicit equations for the dependent variables, viz. core velocity u, radius of the plume b, angle of inclination θ of the plume with respect to x-axis, and core density deficit $\Delta\rho$. After some algebraic operations on the system (Eqs. (20)–(23)) the system of explicit equations follows as:

$$\frac{du}{ds} = \frac{2g\lambda^2\Delta\rho}{\rho_{a0}u}\sin\theta - \frac{2\alpha u}{b}, \tag{24}$$

$$\frac{db}{ds} = 2\alpha - \frac{g\lambda^2\Delta\rho b}{\rho_{a0}u^2}\sin\theta, \tag{25}$$

$$\frac{d\theta}{ds} = \frac{2g\lambda^2\Delta\rho}{\rho_{a0}u^2}\cos\theta, \tag{26}$$

$$\frac{du}{ds} = \frac{(1+\lambda^2)}{\lambda^2}\frac{d\rho_a}{dz}\sin\theta - \frac{2\alpha\Delta\rho}{b}. \tag{27}$$

This nonlinear system can be solved using the Runge–Kutta method with an adaptive step. There are, however, additional quantities which are necessary to plot the plume and which characterize it. These are the coordinates of the plume's core:

$$\frac{dx}{ds} = \cos\theta; \quad \frac{dz}{ds} = \sin\theta \tag{28}$$

and the dilution along the path of the plumes' center (Fan and Brooks, 1966, see Appendix A)

$$S_n(s) = \frac{C_0}{C(s)} = \frac{4\lambda^2u(s)b^2(s)}{(1+\lambda^2)u_0d^2}, \tag{29}$$

where the subscript n indicates that this expression will be used for numerical dilution.

4.2. Initial conditions

In Eq. (29) $C(s)$ is the concentration of any conservative pollutant emerging from the orifice, experiencing the same variations along the trajectory as $\Delta\rho$; $C_0 = C(0)$ is the initial concentration at the orifice; and d ($= 0.1$ m) is the diameter of the orifice.

The integration of the system (Eqs. (24)–(27)) will not commence at the orifice, but close to it, at the end of the zone of flow establishment (ZFE; see Appendix A), for which it has been taken that it is located at a distance $s_0 = 6.2\ d$, as Featherstone (1984) has suggested. There the zone of established flow (ZEF), in which the plume is modeled, starts. The initial velocity at $s = s_0$ is the same as the mean exit velocity at the orifice,

$$u(s_0) = u_0 = \frac{4\phi_0}{\pi d^2} \tag{30}$$

and initial plume's radius (Appendix A) follows from the conservation of momentum flux,

$$b_0 = \frac{d}{\sqrt{2}}. \tag{31}$$

The initial tilt of a buoyant plume is prescribed with the angle of the orifice θ_0 with respect to the horizontal x-axis since within the ZFE the jet does not change its direction,

$$\theta(s_0) = \theta_0. \tag{32}$$

The initial density difference $(\Delta\rho)_0$ at $s = s_0$ needs to be expressed with the difference of densities $(\rho_{a0} - \rho_0)$, where $\rho_{a0} = \rho_a(s = 0)$ is the ambient density, and ρ_0 is the density of an effluent at the orifice. The initial condition follows directly when the expression for the initial concentration C_0 (Appendix A) is expressed with density difference,

$$(\Delta\rho)_0 = \frac{(\rho_{a0} - \rho_0)(1 + \lambda^2)}{2\lambda^2}. \tag{33}$$

The system of equations Eqs. (24)–(27) is integrated from $s_0 = 6.2\ d$ with initial conditions (Eqs. (30)–(33)), accompanied with initial co-ordinates of the core of the plume,

$$x_0 = s_0 \cos\theta_0; \quad z_0 = s_0 \sin\theta_0 \tag{34}$$

and initial dilution

$$S_0 = \frac{2\lambda^2}{(1 + \lambda^2)}, \tag{35}$$

obtained from Eq. (29) with u_0 from Eq. (30) and b_0 from Eq. (31). Initial dilution S_0 lies between 1.15 and 1.18 for λ between 1.16 (Featherstone, 1984) and 1.2 (Fischer et al., 1979). The set of initial conditions (Eqs. (30)–(33)) for the system of equations Eqs. (24)–(27) is, therefore, completed together with the initial values (Eqs. (34) and (35)) for the accompanying equations Eqs. (28) and (29).

There are two options for the coefficient α. The first one is to keep α constant. Fischer et al. (1979) made a distinction between the 'jet' regime (near the orifice, the momentum flux M governs the spreading), in which $\alpha = \alpha_j$, and the 'plume' regime (the buoyancy flux B is important) with $\alpha = \alpha_p$, where the constants have been experimentally determined,

$$\alpha_j = 0.0535 \pm 0.0025; \quad \alpha_p = 0.0833 \pm 0.0042. \tag{36}$$

The jet regime extends from the orifice towards the momentum length scale l_M

$$l_M = \frac{M_0^{3/4}}{B_0^{1/2}} = \left(\frac{\pi}{4}\right)^{1/4} \frac{u_0}{\sqrt{g\Delta\rho/(\rho_{a0}d)}}, \tag{37}$$

where $M_0 = u_0^2(\pi d^2)/4$ is the initial (specific) momentum flux; $B_0 = \phi_0 g\Delta\rho/\rho_{a0}$ is the initial buoyancy flux; and $\phi_0 = u_0(\pi d^2)/4$ the initial volume flux at the orifice. When $s > l_M$ the buoyancy flux takes over the dominant role in spreading. In the southern part of the Gulf of Trieste at a depth of more than 20 m, the ambient density ρ_{a0} is above 1020 and below 1028 kg m^{-3} and varies seasonally with temperature (Malačič, 1991), the effect of salinity variations being negligible. Taking for the initial density of sewage at the orifice as

$$\rho_0 = 1000 \text{ kg m}^{-3} \tag{38}$$

then $\Delta\rho/\rho_{a0}$ is between 0.02 and 0.03. It has been shown in hydraulics for the diffuser 1987 that the discharge velocity $u_0 = (0.70 \pm 0.06)$ m s^{-1} for $\phi_I = 0.1$ m^3 s^{-1}. Taking very wide variations in ϕ_I

and ϕ_{II}, the velocity u_0 is between 0.5 and 2.5 m s^{-1}. From Eq. (37) the lower and upper limits for l_M follow as

$$(l_M)_{min} = 0.3 \text{ m}; \quad (l_M)_{max} = 1.7 \text{ m}. \tag{39}$$

In most cases the elevation of a plume was between 5 and 15 m above the diffusers, meaning that the regime of a buoyant plume dominates and if the option of a constant entrainment coefficient is chosen, then $\alpha = \alpha_p$ from Eq. (36).

In Fischer et al. (1979) a few options in which α is a function of a local Richardson number Ri

$$Ri = \frac{\phi B^{1/2}}{M^{5/4}} = \sqrt{\frac{4\lambda^2\sqrt{2\pi}}{(1+\lambda^2)}\left(\frac{gb\Delta\rho}{\rho_{a0}u^2}\right)} \tag{40}$$

of the plume are registered, among which the following expression

$$\alpha = \alpha_j \exp\left[\left(\frac{Ri}{Ri_p}\right)^2 \ln\left(\frac{\alpha_p}{\alpha_j}\right)\right] \tag{41}$$

looks promising. In Eq. (41) $Ri_p = 0.557$ is a constant Richardson number for a perfect plume without regimes governed by the buoyancy flux alone.

4.3. Model description

A numerical model, which solves the system of equations Eqs. (24)–(27) with initial conditions (Eqs. (30)–(33)), together with accompanying equations Eqs. (28) and (29) with their starting values (Eqs. (34) and (35)), has to have a fundamental property of keeping local errors of all four independent variables below a threshold value at each step Δs along the plume's trajectory. However, then we are faced with another problem, that is a vertical gradient $d\rho_a/dz$ that has to be known at any height z above the orifice, and is not known from data — the step Δs along the plume's trajectory is variable in order to fulfill the conditions for the local errors to be bounded above. For that, a fast cubic spline interpolation method (Press et al., 1988) seems appropriate; with it ρ_a and $d\rho_a/dz$ at height z is readily available from pairs (z_j, $\rho_a[j]$) of input data at each time step. Whole program 'SplinRun' is detailed elsewhere (Malačič, 1998), and only major outlines are summarized here.

A word is necessary about the termination of the program. The main subroutine stops looping by increasing Δs when either $z > 20.7$ m, or the angle of plume's inclination $\theta < 0$ (with $z > 0$). While the former condition is obvious enough, the latter is a tricky one. When a center of a buoyant plume approaches a level of neutral buoyancy, the plume axis is positively inclined ($\theta > 0$) if $-90° < \theta_0 \leq 90°$. Due to inertia the core passes the level of neutral buoyancy in which $\Delta\rho$ changes sign from a positive towards negative and still $u > 0$ (overshooting). Negative buoyancy first decelerates particles in a plume, which finally begin to sink. The height at which $u = 0$ (calculated by interpolation of heights between the two successive steps in which u changes sign) is the numerical maximum height z_{max} of a plume's rise. The radius of the plume increases enormously, and soon after this passage, within the two next steps, a failure of further run of the method manifests itself in achieving $\theta < 0$. We could stop the looping earlier, but in this way we see the evolution of its effectiveness.

4.4. Calibration method

Numerical results have been compared with the verified semi-analytical results, which are mainly grounded on dimensional analysis, and confirmed in laboratory experiments, and are well presented in Fischer et al. (1979).

For a buoyant plume, in which the buoyancy flux dominates and is conserved the height of a rise of a plume is

$$z_{max} = 3.98\left(\frac{B_0}{N^3}\right)^{1/4}, \tag{42}$$

with the initial buoyancy flux $B_0 = g(\Delta\rho/\rho_{a0})\phi_0$.

Fischer et al. (1979) wrote for dilution of a pure buoyant plume emerging from a round orifice into the homogeneous sea:

$$S = 0.089\left(\frac{g\Delta\rho z^5}{\rho_{a0}\phi_0^2}\right)^{1/3}, \tag{43}$$

While for dilution in a stratified sea an expression similar to Eq. (43) was given as

$$S = 0.071\left(\frac{g\Delta\rho z_{\max}^5}{\rho_{a0}\phi_0^2}\right)^{1/3} \quad (44)$$

with a smaller constant of proportionality, and $z_{\max}$ from Eq. (42). The relative deviation S_e of numerical dilution from the experimental one was calculated as

$$S_e = \frac{S_n - S}{S}, \quad (45)$$

where S_n was taken from Eq. (29) and for S Eq. (43) was taken for homogeneous sea, and Eq. (44) for stratified sea. A similar expression to Eq. (45) was utilized for the relative deviation Z_e of model results with respect to experimental ones for the rise height $z_{\max}$. The comparison of rise heights is meaningless for a homogeneous sea, when $z_{\max} = H$.

4.5. Calibration runs

Primary use of the model 'SplinRun' is for a stratified sea, although it can run also for a homogeneous environment. The model has, therefore, been tested for the linear variations of density with height

$$\rho_a = \rho_{a0} - \Gamma z, \quad (46)$$

where for the input pairs (z_j, $\rho_a[j]$) of data (with a height resolution of 0.1 m); $\rho_{a0} = 1027.8232$ kg m^{-3}; and $\Gamma = \rho_0 N^2/g = 0.233$ kg m^{-4} with $N \cong 0.05$ s^{-1}, which meets mean summer stratification in the Gulf of Trieste. Tests were performed also for a homogeneous sea, when it has been supposed that the density is equal to the mean value of densities in the stratified case — between the density at the height of the diffuser and that at the sea surface

$$\rho_a = 1025.48155 \text{ kg m}^{-3}.$$

When model results were compared with the semi-empirical expressions described earlier, the model ran for $\theta_0 = 90°$, simulating the spreading of a vertical buoyant plume. A comparison of model simulations for a linearly stratified environment with semi-empirical (expected) results is shown in Fig. 7. The relative difference of initial dilution in its core S_e and of the maximum height of rise of a plume Z_e is plotted against discharge velocity u_0. The entrainment coefficient is supposed constant (α_p, Eq. (36); left figures) and as a function of local Ri number (right figures). Parameter λ is considered as a parameter with values between 1.1 and 1.2. Interesting to note is that the deviations S_e are smaller for $\alpha =$ constant than those for $\alpha = \alpha(Ri)$. On the other hand, the deviations Z_e from the expected results are higher for $\alpha =$ constant than those for variable α, although differences between the two runs are now smaller. For $\alpha =$ constant Z_e is increasing with u_0 from 2% ($u_0 = 0.5$ m s^{-1}) to 12% ($u_0 = 2.5$ m s^{-1}), nearly independently of λ. For $\alpha = \alpha(Ri)$ Z_e is monotonously decreasing with u_0, from 5 to 2%. For smaller values of u_0 (≤ 1.0 m s^{-1}), which are quite common for both diffusers, simulations with $\alpha =$ constant are preferred; in these cases S_e is decreasing with u_0 for $\lambda = 1.1$ and increasing with u_0 for $\lambda = 1.17$ and for $\lambda = 1.2$. For $\lambda =$ 1.13–1.15 S_e reaches minimum at certain speed u_0. For low discharge velocities best results were obtained for $\lambda = 1.16$ (Featherstone, 1984). Over the whole range of u_0, however, the best results were achieved for $\lambda = 1.14$. In this case, S_e is small, i.e. below 2.8%. Such small deviation from expected values is ideal for the numerical model. S_e represents the absolute value of relative deviation according to Eq. (45). At $u_0 = 0.5$ m s^{-1} numerical estimate $S = 46.8$, while the expected value calculated with Eq. (44) is higher, namely 47.7. At $u_0 = 2.5$ m s^{-1} numerical estimate for $S = 32.8$, while the expected dilution equals 31.9. At $u_0 = 1.5$ m s^{-1} the match is nearly perfect (up to 0.2%).

In testing the numerical model for dilution of a buoyant plume in a homogeneous sea only the deviation S_e was studied, since now the plume reaches the sea-surface. Fig. 8 shows that if $\alpha =$ constant S_e is increasing with u_0 at $\lambda = 1.2$, while for $\lambda = 1.13$–1.14 S_e is relatively low and nearly independent of u_0. When $\lambda = 1.14$, S_e is between 2 and 4.5% for u_0 between 0.5 and 2 m s^{-1}. However, for high speeds ($u_0 = 2.5$ m s^{-1}) $S_e = 7\%$. The match of the model with expected results is worse for $\alpha = f(Ri)$. $S_e > 6\%$ for all values of λ and there is no significant dependence on u_0. We arrive at the conclusion that $\lambda = 1.14$ is an acceptable choice also for modeling the spreading of a

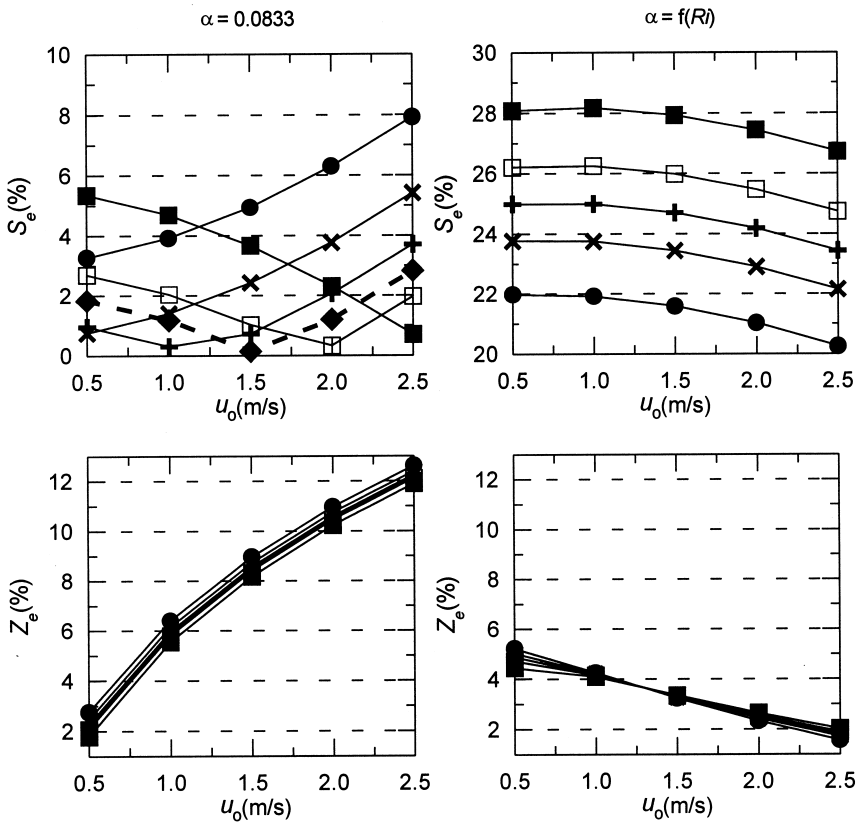

Fig. 7. Absolute deviations of model results from the 'expected' ones of dilution S_e (top) and of maximum height of plume's rise Z_e (bottom) for linear profile of ambient density, according to Eq. (46) (see text). Left, runs for $\alpha = \alpha_p$; right, $\alpha = \alpha(Ri)$, as in Eq. (41). Parameter λ has values of 1.10 (■), 1.13 (□), 1.14 (◆), 1.15 (+), 1.17 (×) and 1.20 (●). Best results are obtained for $\lambda = 1.14$ (dashed).

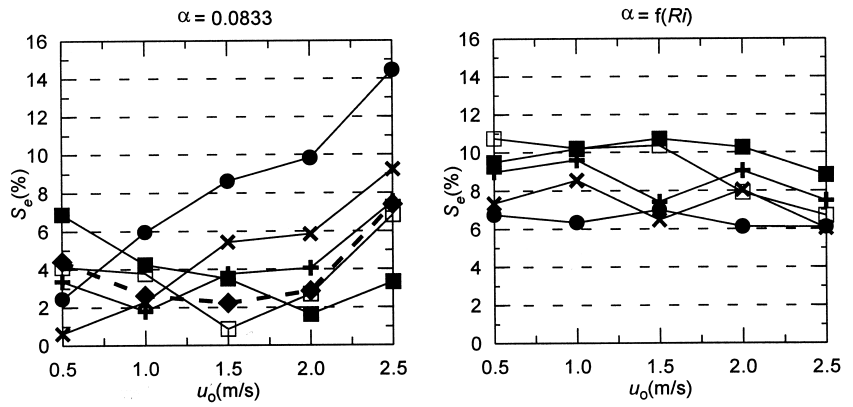

Fig. 8. Absolute values of relative deviations of numerical dilution from the expected values for a homogeneous environment (see text). Left, runs for $\alpha = \alpha_p$; right, $\alpha = \alpha(Ri)$, as in Eq. (41). Values of λ are 1.10 (■), 1.13 (□), 1.14 (◆), 1.15 (+), 1.17 (×) and 1.20 (●). Again, best results were chosen for $\lambda = 1.14$ (dashed).

buoyant plume in a homogeneous environment for a whole range of discharge velocities.

It follows from model tests that a match with the expected results is better for runs with $\alpha = \alpha_p$ than that with α varying with a local *Ri* number. This was anticipated since the 'expected' results (Eqs. (42)–(44)) are those for a pure buoyant plume. The model calibration ended in such a way that the model parameters were held constant; $\alpha = \alpha_p$ and $\lambda = 1.14$ during runs for applications.

5. Model results

5.1. Variations of initial conditions

Once the model parameters α_p and λ were determined from model testing, the model results were examined as a function of initial conditions. In case of the outfall at Piran, the initial radius of the discharged jet was determined by the diameter of the diffuser's orifice (0.1 m); therefore, in all sensitivity runs b_0 was held fixed, and the remaining three initial conditions u_0, θ_0 in $(\Delta\rho)_0$ are to be varied. However, of them, $(\Delta\rho)_0$ is the one which varies little; according to Eq. (33) it is proportional to the density difference $\rho_{a0} - \rho_0$. Density ρ_0 varies very little, the previously assumed initial value for ρ_0 (1000.0 kg m^{-3}) in test runs is sufficient. Sea density at the depth of the diffusers ρ_{a0} varies more (between 1025 and 1028 kg m^{-3}) but on a larger time scale (days). Therefore, $\rho_{a0} - \rho_0$ is between 25 and 31 kg m^{-3}, deviating for $\pm 10.7\%$ around ρ_{a0} in Eq. (46). In model runs it has been taken that $(\Delta\rho)_0 = [(1 + \lambda^2)/2\lambda^2]$ 27.82 kg m^{-3} = 24.76 kg m^{-3} for $\lambda = 1.14$. Therefore, model sensitivity is to be examined only for two initial conditions, θ_0 and u_0.

Initial inclinations of buoyant jets θ_0 emerging from orifices of diffusers in Piran bay were described in the section on the diffusers' hydraulics. It is, of course, constant with time, and for all orifices it should be $\theta_0 = 0$. Diving inspections showed that the diffuser 1987 has θ_0 variable along the pipe, from $\pm 5°$ up to $\pm 30°$, while the span of values for the 1976 diffuser is even higher; from $\pm 45°$ to $\pm 90°$. This uncertainty in knowledge of θ_0 for individual orifice suggests the study of model sensitivity to θ_0. Contrary to θ_0 discharge velocities u_0 vary with time, in a rhythm of variations of discharge rates of flows ϕ_I and ϕ_{II}; Fig. 2 gives also an indication of daily variations of u_0. In model runs u_0 varied from 0.5 to 2 m s^{-1} with a step of 0.5 m s^{-1}, while θ_0 varied from -60 to 90° with a step of 30°. Unfortunately, it is beyond the capabilities of this model to simulate the spread of pollutant for $\theta_0 = -90°$, when the initial direction of jet is directly downward.

5.2. Sensitivity of results to initial conditions

Model results were observed for simulations of the spreading of a buoyant plume in mean summer conditions (linearly stratified ambient, according to Eq. (46)). In Fig. 9 trajectories are shown together with their widths (radius b) for different values of u_0 (different plots) and θ_0. The orifice is always located in coordinate origin, in immediate vicinity of which the ZFE was supposed first (within a distance of $6.2d$), after which the ZEF commenced with numerical simulations of spreading.

Model results of spreading in a linearly stratified sea are summarized in Table 1. Dilution S at the end of a plume's rising is the smallest at simulations with the highest discharge velocity, while the highest dilution is reached for small discharge velocities. Dilution ranged between values above 34 and below 48. These results swiftly lead us to conclude that dilution at the end of a rising plume is only slightly dependent on θ_0, the differences between dilutions for θ_0 ranging from $-60°$ to 90° when u_0 is held fixed are lower than 6%. Dilution is far more sensitive to variations of u_0:S varies up to 30% for u_0 between 0.5 and 2.0 m s^{-1}, when θ_0 is held fixed.

Contrary to findings for sensitivity of dilution are the results for maximum rise height z_{max} of a plume, which is much more sensitive to variations of θ_0 than S. Relative variations of z_{max} due to variations in θ_0 are between 23 ($u_0 = 0.5$ m s^{-1}) and 35% ($u_0 = 2.0$ m s^{-1}), where in case of θ_0 being fixed they are close to 18%.

Model shows (Table 1) that under summer stratified conditions the initial dilution varies between 34 ($u_0 = 2.0$ m s^{-1}, $\theta_0 = 90°$) and 47 ($u_0 = 0.5$ m s^{-1}, $\theta_0 = 0°$). The sewage plume finds its neutral

buoyancy below the mid-depths of the water column, between 5.5 and 8 m above the diffuser, and that the whole rise of a plume is completed in less than 34 s.

6. Discussion

When the hydraulics of diffusers is addressed, it is worth mentioning that in planning the diffusers the calculation of hydraulics is usually done for the nominal flow rate which is to be expected under excess load (e.g. severe rain storm for a sewerage system of mixed type, tourism during the summer period). Under such circumstances the diffuser pipes are fully loaded with wastewater, which emerges into the sea from all orifices. The hydraulic calculus used in section two is good at reproducing this kind of hydraulics regime. However, the classic hydraulic calculus used in section two still gives the bulk estimates of spreading from the orifices when the flow rate of effluent is low and the seawater enters in the diffuser. One of the major problems encountered in this case is the friction between the sewage and seawater in the pipe, which certainly deserves full attention in future studies. We may summarize

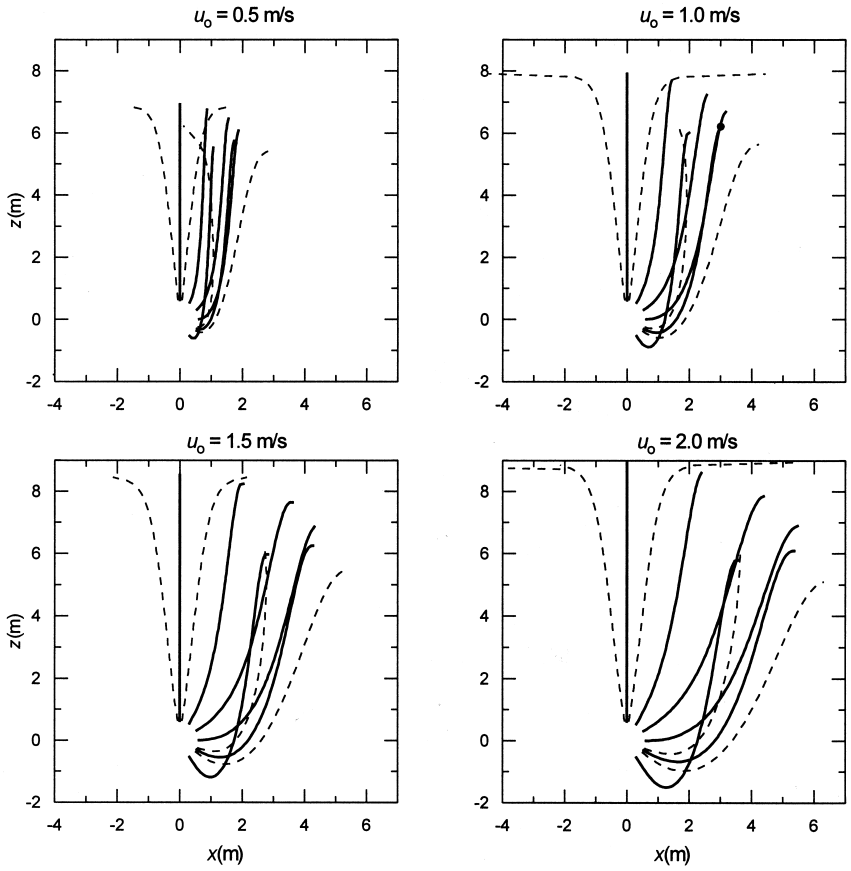

Fig. 9. Trajectories of a buoyant plume (full lines), together with their widths (radius b). Discharge velocities u_0 are written above each plot. The trajectories are drawn for initial inclinations $\theta_0 = -60°$ to 90°, with a step of 30°. Lines of jet width are shown only for $\theta_0 = -30°$ and $\theta_0 = 90°$. Horizontal dashed lines for $\theta_0 = 90°$ indicate a horizontal spread of a plume in a neutral layer. A dot marks the end of a trajectory, when it is overlapped with another one. Buoyant plume with initial density difference $(\Delta\rho)_0 = 24.76$ kg m^{-3} spreads into a linearly stratified density field (Eq. (46)) from an orifice ($d = 0.1$ m) that is surrounded with a ZFE within a distance of $6.2d$ (blanked).

Table 1
Summary of model results — model sensitivity to initial conditions u_0 and θ_0[a]

u_0 (m s^{-1})	Minimum (S)	θ_0 (°)	Maximum (S)	θ_0 (°)
0.5	46.9	−60	47.1	0
2.0	34.2	90	36.1	0
	Minimum (z_{max}) (m)		Maximum (z_{max}) (m)	
0.5	5.5	−60	6.9	90
2.0	5.8	−60	8.3	90
	Minimum (t_{max}) (s)		Maximum (t_{max}) (s)	
0.5	31.2	90	32.7	−60
2.0	28.2	90	34.0	−60

[a] Runs were performed for simulations of a buoyant jet spreading from a round orifice in a linearly stratified sea, according to Eq. (46), t_{max} is the time in which the core of a plume reaches height z_{max}.

that this inconvenience is a problem of sea-water intrusion (Charlton, 1985).

When turning to initial dilution outside of a diffuser, we first need to clarify the range (0.5–2.5 m s^{-1}) of discharge velocity u_0 for which the model was tested. As was clear from the section on hydraulics the value 0.5 m s^{-1} is close to the average value for u_0 of both diffusers. The best agreement of model results with semi-empirical results is then obtained for $\lambda = 1.16$ (Figs. 7 and 8) that was used by Featherstone (1984). However, the model of initial dilution was also developed and applied for design purposes of future diffuser(s) that are to be constructed in the neighboring Bay of Koper (Fig. 1). The population equivalent there is about 2.5 times higher than that for Piran. The sewage velocity through the submarine pipe, which needs to provide the diffuser with self-cleaning capacity, would be increased accordingly. The discharge velocities would, therefore, also be increased, and the preferred value for $u_0 \geq 1$ m s^{-1}. For the whole range of u_0 the best model results were found for $\lambda = 1.14$, although S_e for both values of λ differs for 2% at most.

Needless to say, the phase of initial rising of a buoyant plume is quickly over — the core of a plume reaches z_{max} after a time t_{max}, which is between 28 and 34 s. Numerical simulations demonstrated that θ_0 influences the variations of t_{max} between 5.6 ($u_0 = 0.5$ m s^{-1}) and 18.8% ($u_0 = 2.0$ m s^{-1}). However, when θ_0 is fixed (e.g. $\theta_0 = 90°$), and the initial velocity varies, the influence of u_0 on t_{max} is smaller (less than 8.2%). Another interesting numerical observation was noted: at high speed u_0, the core velocity u drops sharply to much smaller values within an interval of a few seconds (< 5 s), after which it decreases further with time, nearly linearly towards zero. At smaller initial velocities u_0, the initial drop of u is lower, but the course of further decrease of u is very similar to the one for high values of u_0. This peculiarity is beyond the scope of this paper, but it deserves to be studied further.

Numerical results about the timing of initial rise lead to the conclusion that for a buoyancy frequency $N = 0.05$ s^{-1} the rising time is about 30 s and that in a first approximation

$$Nt_{max} \approx 1.5. \quad (47)$$

It follows from Eq. (47) that the N^{-1} is a suitable estimate for a rising time. Fonseka et al. (1998) recently obtained from laboratory observations of a buoyant fluid, which was suddenly ejected into a stratified fluid, that $Nt_{max} \sim 4$–5. Their experiments well simulate a sudden discharge of a puff of effluent, but this dynamics is different from that of a continuous release of pollutant (e.g. different entrainment of ambient fluid through different boundary areas).

Another peculiarity found with numerical observations about the width of a buoyant plume also deserves attention. The radius b of a plume increases rapidly (for a factor of 100) at small distance ($\Delta s < 0.1$ m), just before the end of the rising is reached. Horizontal dashed lines, which would indicate this horizontal widening, were not plotted in Fig. 9 (except for $\theta_0 = 90°$), so as not to reduce the clarity of the plots. Final plotted widths of plumes are the ones obtained from the last but one numerical step. All values of b are below 2.3 m. Since for diffusers in the Bay of Piran, the distance between two consecutive alternating orifices is 10 m, the choice of simulation of individual plumes emerging from a port of the diffuser into a stagnant stratified sea is justified. Before entering into a neutral layer, individual plumes, which spread in a stratified sea with low currents, are most certainly not merged.

Model results were tested with the expressions for dilution and rise height of an ideal buoyant plume. The latter is a good approximation for plumes which spread high enough: $z_{max} \gg l_M$, where l_M follows from Eq. (37). This means that for the Gulf of Trieste, when the rise height $z_{max} \leq 5$ m, the discrepancy between the ideal buoyant plume and real plume is meaningful, the effluent behaves at first as a jet with dominant momentum flux, and it turns later into a buoyant plume, for which the flux of buoyancy governs its spreading. Therefore, larger deviations of model results from those of an ideal buoyant plume do not necessarily mean that the model is invalid — instead the testing conditions could be inappropriate.

There are two ways in which the numerical modeling of initial dilution and spreading of sewage, which comes out of the diffuser's ports, could be oriented — modeling of sewage spreading out of a point source (e.g. round orifice), or modeling of dilution of sewage emerging from a line source. To examine which way would be a better choice in our case, a few nondimensional numbers, which characterize the initial dilution, have to be defined first as was done by Roberts et al. (1989a).

Let us suppose that the whole diffuser is approximated as a finite line source, then the buoyant length scale $l_B = B^{1/3}/N$, where $B = g'q$, is the buoyancy flux per diffuser's length; $g' = g(\Delta\rho)_0/\rho_{a0}$ is the reduced gravity acceleration; $(\Delta\rho)_0 = \rho_{a0} - \rho = 27.8$ kg m^{-3} is the difference between ambient and sewage density, and $q = \phi/L$ is the discharge rate per diffuser's length. Since $\Delta x = 10$ m and $(l_B)_{max} = H$, the first nondimensional number $(\Delta x/l_B) \geq 0.5$, where the lower boundary is achieved during the winter period. During the summer period ($N = 0.05$ s^{-1}) and extreme discharge rate ($q = 0.2$ m^3 s^{-1} 100 m^{-1}) $l_B = 1.6$ m; therefore, $(\Delta x/l_B) \geq 6$ where u_0 is the outflow velocity through round ports of diameter d (0.1 m). The ratio l_M/l_B is always < 0.3, where $l_M (= u_0 q)$ is the momentum length scale.

The second nondimensional number is of a type of ambient Froude number which shows the influence of currents, $F = u_a^3/B$ (Roberts et al., 1989a), where u_a is the current speed. Tides in the northern Adriatic are of mixed type and peak tidal currents are about 0.1 m s^{-1} (Malačič and Viezzoli, 1998). Although currents of other origins (mainly density-driven and wind-driven currents) also influence the spreading, we will make a good estimate by taking $u_a \leq 0.2$ m s^{-1}. While the lower limit of $F = 0$, for the upper limit of F we need the lower limit of B. We may expect that $\phi \geq 0.03$ m^3 s^{-1} (Fig. 2), then $q_{min} = 3 \times 10^{-4}$ m^2 s^{-1} and $B_{min} = 7.96 \times 10^{-5}$ m^3 s^{-3}, therefore $F \leq 100$.

The line source is certainly a better choice when looking at the buoyant field from the distance over which the waste-field has already been formed and is further influenced by advection/dispersion processes. When $\Delta x/l_B \cong 6$, as it is during the summer period, then the model of individual plumes becomes a priority for a closer look at spreading. The effect of port spacing (and momentum flux of sewage) has been studied with laboratory experiments by Roberts et al. (1989b). We shall focus on their results, which were found for low momentum fluxes ($l_M/l_B < 0.2$). When there is no current ($F = 0$), 'widely' spaced individual plumes emerging from ports ($\Delta x/l_B \geq 6$), which is the case in the Gulf of Trieste during the summer, do not merge before entering the horizontal layer. Roberts et al. (1989b) conclude that for a stagnant fluid the point plume formulas for

dilution and rise height will apply for a stagnant fluid and for $\Delta x/l_B \geq 1.92$.

When currents are present, the situation changes: the plumes merge faster and can no longer be taken anymore to be isolated. The arrested upstream horizontal wedge of pollutant is swept downstream for $F \geq 0.04$ (Roberts et al., 1989c). As Roberts et al. (1989b) concluded the point plume expressions could be used only in low current conditions (and high stratification). Since our primary goal is to estimate the mixing and spreading in the worst case scenario (no currents which increase dilution), i.e. to be on the safe side of planning future diffusers, and since the circulation during the season is relatively weak (peak tidal currents of 0.1 m s^{-1}), a numerical model for a plume emerging from a single round port of a diffuser in a stagnant environment with complicated stratification certainly sounds meaningful.

7. Conclusions

Simulations of the spreading of a buoyant plume in a homogeneous and stratified calm environment showed that the agreement of model results with the expected ones for the ideal buoyant plume was better when it was supposed that the coefficient of entrainment α was held constant, at a value equal to the one observed for plumes. For discharge velocities between 0.5 and 2.5 m s^{-1} best results were obtained when the ratio between the radius of velocity profile and the radius of density profile $\lambda = 1.14$.

Simulations of plume spreading in stratified conditions, similar to those for the Gulf of Trieste, demonstrated that the initial dilution is between 34 ($u_0 = 2.0$ m s^{-1}, $\theta_0 = 90°$) and 47 ($u_0 = 0.5$ m s^{-1}, $\theta_0 = 0°$), which is within the expected dilution according to UNEP (1995) recommendations (between 10 and 1000). The latter are, however, meant for a total decrease of bacteria, including the die-off when bacteria are exposed to UV light, and the shock of living conditions, which they experience once arriving in sea-water. We may conclude that simulations confirmed the relative efficiency of diffusers, even in conditions which deteriorate their hydraulics. The shallowness of the Gulf of Trieste is a deficiency, which limits the initial dilution. The expressions Eqs. (43) and (44) for dilution of a buoyant plume in a homogeneous and stratified sea demonstrate that dilution increases with height proportionally to $z^{5/3}$ — in the southern part of the Gulf of Trieste $z < 22$ m.

Sensitivity analysis of the model revealed that initial inclination θ_0 of a buoyant jet with respect to the horizontal axis has low influence on dilution ($< 6\%$), which is much more sensitive to variations of initial (discharge) velocity. Dilution varies up to 30% when u_0 increases from 0.5 to 2 m s^{-1}. In contrast, the maximum rise height of a plume is more dependent on θ_0 than on u_0. The rise height is the smallest for small initial velocities of jets facing downwards ($z_{max} = 5.5$ m at $u_0 = 0.5$ m s^{-1} and $\theta_0 = -60°$). It reaches its maximum for large upward initial velocities ($z_{max} = 8.3$ m at $u_0 = 2.0$ m s^{-1} and $\theta_0 = 90°$). Relative variations of z_{max} with θ_0 are below 35% (then $u_0 = 2.0$ m s^{-1}), while they are much lower (18%) when u_0 changes from 0.5 to 2 m s^{-1}. All simulations of spreading in typical summer stratification of the Gulf of Trieste ($N = 0.05$ s^{-1}) clearly demonstrated that the effluent would settle at a height between 5.5 and 8.3 m above the diffusers, never reaching the sea surface (about 20 m above the diffusers), which is another indication of the advantage of discharging the effluent through diffusers.

Since the radius of buoyant plumes, just one step (< 0.1 m) before they reach z_{max}, is smaller than 2.3 m, the initial supposition that individual plumes do not merge before entering a buoyant layer was correct. The orifices are at a distance of 10 m and the choice of developing the numerical model of spreading of effluent from a round orifice was a good one. However, as soon as the waste field formed out from individual plumes is to be studied, one needs to resolve for a line source model (Roberts and Wilson, 1990). The initial dilution during the rising phase ends within 30 s, certainly in a period shorter than a few minutes under any stratified conditions.

Acknowledgements

The author wish to thank Danijela Kleva for providing us with the data about the sewage treatment plant, to Janez Forte for laboratory experiments and especially to Tihomir Makovec for his technical help. Video tapes of diver's inspections were kindly provided by Ugo Fonda. The project L1-8882 has been co-sponsored by the Ministry of Science and Technology of Slovenia and by the municipial Public company 'Okolje Piran'.

Appendix A

A link between the changes of fluxes ϕ and B follows from Eq. (16): along the path ds of the plume's trajectory $\mathrm{d}\phi = E\,\mathrm{d}s$, while the specific mass flux changes for $\mathrm{d}\psi = E\rho_a\,\mathrm{d}s$ (Fig. 6). The subtraction of $\mathrm{d}\psi/\mathrm{d}s - \rho_{a0}\,\mathrm{d}\phi/\mathrm{d}s$, where ψ and ϕ are from Eq. (14) yields

$$\frac{\mathrm{d}}{\mathrm{d}s}\left[\int_A (\rho - \rho_{a0})u\;\mathrm{d}A\right] = (\rho_a - \rho_{a0})E. \tag{A.1}$$

Let us write $\rho - \rho_{a0} = \rho_a - \rho_{a0} - \Delta\rho$, the left-hand side of (Eq. (A.1)) equals to $\phi\,\mathrm{d}\rho_a/\mathrm{d}s - (\rho_{a0}/g)\mathrm{d}B/\mathrm{d}s + (\rho_a - \rho_{a0})\mathrm{d}\phi/\mathrm{d}s$, where again Eq. (14) has been applied for ϕ and B. When invoking Eq. (16), Eq. (A.1) simplifies to Eq. (19).

The expression (Eq. (29)) for dilution has been already introduced by Fan and Brooks (1966). The specific mass flux of a pollutant through a tube of height ds, thickness dr and radius r is $\mathrm{d}\psi_c = \mathrm{d}m_c/\mathrm{d}t = 2\pi Cru\,\mathrm{d}r$, the distribution of velocity is given by Eq. (17), as well as the distribution of concentration C, which follows $\Delta\rho$. The specific mass flux of a pollutant

$$\Psi_c = \pi\frac{\lambda^2 C(s)u(s)b^2(s)}{1+\lambda^2} \tag{A.2}$$

is conserved — there is no entrainment of a pollutant from the ambient fluid, therefore,

$$C(s)u(s)b^2(s) = C_0^* u_0 b_0^2, \tag{A.3}$$

where $C_0^* = C(s_0)$, $u_0 = u(s_0)$ and $b_0 = b(s_0)$ are the concentration, core velocity and radius of the plume at distance s_0 from the orifice, respectively, — ZFE ends there, and ZEF, which is modeled here, begins. Fischer et al. (1979) described this transition of a jet near the orifice from one regime into another. For C_0^* as a function of C_0, the concentration at the orifice, a conservation of pollutant within the ZFE is utilized; at the orifice the specific mass flux is

$$C_0\phi_0 = C_0\frac{\pi u_0 d^2}{4} \tag{A.4}$$

Since the specific flux of momentum is also conserved within the ZFE, $M = M_0 = \pi u_0^2 d^2/4 = M(s_0)$, where for the latter (Eq. (18)) can be applied $M(s_0) = \pi u^2(s_0)b_0^2/2$. Within the ZFE the core velocity is nearly constant and equal to the discharge velocity (from where Eq. (30) follows), the initial radius is therefore $b_0 = d/2^{1/2}$ (Eq. (31)). The specific mass flux (Eq. (A.4)) equals the one at the end of ZFE (Eq. (A.2)) with $s = s_0$ and b_0 from Eq. (31). In this way the concentration C_0^* follows

$$C_0^* = \frac{C_0(1+\lambda^2)}{2\lambda^2}, \tag{A.5}$$

and from here the expression (Eq. (33)) for the initial density difference.

If ψ_c in Eq. (A.2) is written as a product $\langle C\rangle\phi$, in which $\langle C\rangle$ is the concentration averaged over the flux, while ϕ follows from Eq. (18), then

$$\langle C\rangle = \frac{\Psi_c}{\phi} = \frac{\lambda^2}{(1+\lambda^2)}\,C(s), \tag{A.6}$$

where $C(s)$ is the core concentration of a plume. $\langle C\rangle$ is smaller than $C(s)$ for a factor between 0.57 ($\lambda = 1.16$) and 0.59 ($\lambda = 1.2$).

There are several definitions of dilution, most of them are described in Fischer et al. (1979). The first one defines dilution as a ratio between volume fluxes:

$$S_c = \frac{\phi}{\phi_0} = \frac{C_0}{\langle C\rangle}, \tag{A.7}$$

where the r.h.s. follows from the conservation of the specific mass flux $\psi_c = \int Cu\;\mathrm{d}A = \langle C\rangle Q = C_0 Q_0$, since no pollutant entrains into the plume. For volume flux ϕ the expression in Eq. (18) is utilized, and $\phi_0 = \pi u_0 d^2/4$, from which it follows,

$$S_c = \frac{4ub^2}{u_0 d^2}. \tag{A.8}$$

Fischer et al. (1979) wrote ϕ (in their notation μ) for a buoyant plume as a function of B and z, which leads to,

$$S_c = 0.15\,\frac{B^{1/3}z^{5/3}}{\phi_0} = 0.15\left(\frac{g(\Delta\rho)_0 z^5}{\rho_{a0}\phi_0^2}\right)^{1/3}. \tag{A.9}$$

This expression invokes the conservation of $B = B_0 = g(\Delta\rho/\rho_{a0})\phi_0$, with $(\Delta\rho)_0 = \rho_{a0} - \rho_0$. The conservation is strictly valid for a homogeneous sea (see the expression in Eq. (19)). The relative error of the constant of proportionality in Eq. (A.9) is 10%.

For the model calibration, a slightly different definition of dilution is used (Fan and Brooks, 1966)

$$S = \frac{C_0}{C(s)} = \frac{\lambda^2}{(1+\lambda^2)}\,\frac{C_0}{\langle C\rangle} = \frac{\lambda^2}{(1+\lambda^2)}\,S_c \tag{A.10}$$

in which for the r.h.s. the Eqs. (A.6) and (A.7) were utilized. The proportionality factor $\lambda^2/(1+\lambda^2)$ was already estimated for $\langle C\rangle$ in Eq. (A.6). Dilution as defined with Eq. (A.6) can also be expressed with the plume's radius and core velocity. By inserting in Eq. (A.3) b_0 from Eq. (31) and C_0^* from Eq. (A.5) dilution S yields in a form Eq. (29). Dilution in Eq. (43), however, is in concordance with Eq. (A.10), where S_c follows from Eq. (A.9), the constant of proportionality $0.089 = 0.15\,\lambda^2/(1+\lambda^2)$ with $\lambda = 1.2$. Dilution calculated with Eq. (43) means that dilution is defined as the ratio between the initial concentration and the core concentration at the top of a buoyant plume, which is located at the sea-surface for a homogeneous sea.

References

Avčin, A., Vrišer, B., Vukovič, A., 1979. Ecosystem modifications around the submarine sewage outfall from Piran sewage system. Slovensko morje in zaledje (In Slov.) 2/3, 295–299.

Brooks, N.H., 1970. Ocean disposal. Notes for the Fifteenth Summer Institute in Water Pollution Control, Course on Stream and Estuarine Analysis. Manhattan College, May 1970, p. 43.

Chadwick, A., Morfett, J., 1986. Hydraulics in Civil Engineering. Harper Collins, London, p. 492.

Charlton, J.A., 1985. Sea outfalls. In: Novak, P. (Ed.), Developments in Hydraulic Engineering, 3. Elsevier, London, pp. 79–127.

Douglass, J.F., Gasiourek, J.M., Swaffield, J.A., 1979. Fluid Mechanics, third ed. Longman, New York, p. 819.

Faganeli, J., 1982. Nutrient dynamics in seawater column in the vicinity of Piran submarine sewage outfall (North Adriatic). Mar. Pollut. Bull. 13, 61–66.

Fan, L.N., Brooks, N.H., 1966. Horizontal jets in stagnant fluid of other density. J. Hydraul. Divn. ASCE 92, 423–429.

Featherstone, R.E., 1984. Mathematical models of the discharge of wastewater into a marine environment. In: James, A. (Ed.), An Introductory to Water Quality Modelling, first ed. Wiley, Chichester, pp. 150–162.

Fischer, H.B., List, E.J., Koch, R.C.Y., Imberger, J., Brooks, N.H., 1979. Mixing in Inland and Coastal Waters. Academic Press, New York, p. 483.

Fonseka, S.V., Fernando, H.J.S., van Heijst, G.J.F., 1998. Evolution of an isolated turbulent region in a stratified fluid. J. Geophys. Res. 103 (C11), 24857–24868.

Lalić, O., 1987. Hidravlični izračun difuzorja in izračun dilutivnih procesov. In: Maver, J. (project leader), Podmorski izpust Piran. Project Report of Komunalno podjetje Piran, Projektiva inženiring. Rep. no. 14/86. Piran, April 1987.

Malačič, V., 1991. Estimation of the vertical eddy diffusion coefficient of heat in the Gulf of Trieste (Northern Adriatic). Oceanol. Acta 14, 23–32.

Malačič, V., 1998. Geofizikalno-ekološki pristop k disperziji odplak piranskega izpusta. National Institute of Biology, Marine Biological Station Piran, Report no. 2, p. 43.

Malačič, V., Viezzoli, D., 1998. Tidal dynamics in the Gulf of Trieste — northern Adriatic. Rapp. Comm. Int. Mer Médit., 35. Dubrovnik, Croatia, pp. 172–173.

Malačič, V., Vukovič, A., 1997. Preliminary results of the submarine outfall survey near Piran (northern Adriatic sea). In: Kranjc, A. (Ed.), Tracer Hydrology 97. Balkema, Rotterdam, pp. 263–268.

Malej, A., 1980. Effects of Piran underwater sewage outfall upon surrounding coastal ecosystem (North Adriatic). Journées Étud. Pollutions, 5, C.I.E.S.M., Cagliari, Italy, pp. 743–748.

Malej, A., Mozetič, P., Malačič, V., Turk, V., 1997. Response of summer phytoplancton to episodic meteorological events (Gulf of Trieste). P. S. Z. N. I. Mar. Ecol. 18, 273–288.

Mozetič, P., Malačič, V., Turk, V., 1999. Ecological characteristics of seawater influenced by sewage outfall. Annales 9 (2), 177–190.

Olivotti, R., Faganeli, J., Malej, A., 1986. Impact of 'organic' pollutants on coastal waters, Gulf of Trieste. Water Sci. Technol. 18, 57–86.

Press, W.H., Teukolsky, S.A., Vetterling, W.T., Flannery, B.P., 1988. Numerical Recipes in C. Cambridge University Press, Cambridge, p. 735.

Roberson, J.A., Crowe, C.T., 1997. Engineering Fluid Mechanics, sixth ed. Wiley, New York, p. 688.

Roberts, P.J.W., Wilson, D., 1990. Field and model studies of ocean outfalls. Hydraulics Engineering Proceedings, National Conference. HY Div/ASCE, San Diego, pp. 1–7.

Roberts, P.J.W., Snyder, W.H., Baumgartner, D.J., 1989a. Ocean outfalls. I. Submerged wastewater formation. J. Hydraul. Eng. ASCE 115, 1–25.

Roberts, P.J.W., Snyder, W.H., Baumgartner, D.J., 1989b. Ocean outfalls. III. Effect of diffuser design on submerged wastefield. J. Hydraul. Eng. ASCE 115, 49–70.

Roberts, P.J.W., Snyder, W.H., Baumgartner, D.J., 1989c. Ocean outfalls. II. Spatial evolution of submerged wastefield. J. Hydraul. Eng. ASCE 115, 26–47.

Swamee, P.K., Jain, A.K., 1976. Explicit equations for pipe-flow problems. J. Hydraul. Div. ASCE 102, 657–664.

Turner, J.S., 1986. Turbulent entrainment: the development of the entrainment assumption, and its application to geophysical flows. J. Fluid Mech. 173, 431–471.

UNEP, 1995. Guidelines for Submarine Outfall Structures for Mediterranean Small and Medium-Sized Coastal Communities. Working document, UNEP(OCA)/MED WG. 89/Inf. 6, p. 34.